ACS chemical biology

Letters

pubs.acs.org/acschemicalbiology

Elastase-like Activity Is Dominant to Chymotrypsin-like Activity in 20S Proteasome's β5 Catalytic Subunit

Dennis Bensinger,[†,∥] Theresa Neumann,[†,∥] Christoph Scholz,[†] Constantin Voss,[†] Sabine Knorr,[‡] Ulrike Kuckelkorn,[§] Kay Hamacher,[‡] Peter-Michael Kloetzel,[§] and Boris Schmidt*[,†]

[†]Clemens Schöpf Institute for Organic Chemistry & Biochemistry, Technische Universität Darmstadt, Alarich Weiss Str. 4-8, 64287 Darmstadt, Germany

[‡]Computational Biology & Simulation, Technische Universität Darmstadt, Schnittspahnstr. 10, 64287 Darmstadt, Germany

[§]Institute of Biochemistry CCM, Charité Universitätsmedizin Berlin, Charitéplatz 1/Virchowweg 6, 10117 Berlin, Germany

Supporting Information

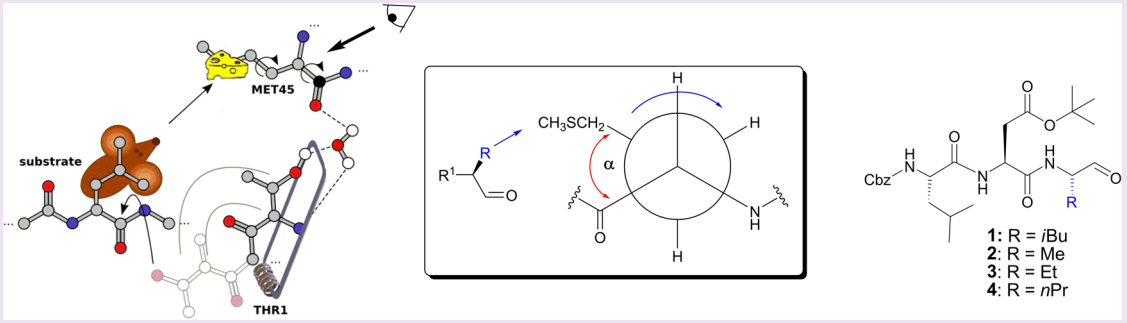

ABSTRACT: The ubiquitin/proteasome system is the major protein degradation pathway in eukaryotes with several key catalytic cores. Targeting the β5 subunit with small-molecule inhibitors is an established therapeutic strategy for hematologic cancers. Herein, we report a mouse-trap-like conformational change that influences molecular recognition depending on the substitution pattern of a bound ligand. Variation of the size of P1 residues from the highly β5-selective proteasome inhibitor **BSc2118** allows for discrimination between inhibitory strength and substrate conversion. We found that increasing molecular size strengthens inhibition, whereas decreasing P1 size accelerates substrate conversion. Evaluation of substrate hydrolysis after silencing of β5 activity reveals significant residual activity for large residues exclusively. Thus, classification of the β5 subunit as chymotrypsin-like and the use of the standard tyrosine-containing substrate should be reconsidered.

The proteome, the entirety of proteins in an organism at a given time, underlies a complex and dynamic equilibrium between protein synthesis and degradation. In eukaryotes, the ubiquitin/proteasome system (UPS) is the major ATP-dependent degradation pathway. Ubiquitin, a small 8 kDa protein, is covalently attached to a substrate, which is subsequently recognized and degraded to small fragments by the 26S proteasome.[1] This 26S proteasome is a 2.5 MDa multicatalytic threonine protease complex that consists of two regulatory 19S subunits, which recognize and unfold ubiquitinylated substrates, and a cylinder-shaped core particle (CP), the 20S proteasome, which harbors the active sites. The CP consists of 28 subunits with an $\alpha_7\beta_7\beta_7\alpha_7$ symmetry and features six active sites bearing three different substrate specificities, classified as caspase-like activity (C-like, β1) because of its tendency to cleave peptides on the carboxyl side of glutamyl or aspartyl side chains, the trypsin-like activity (T-like, β2) due to the cleavage after basic P1 residues, and the chymotrypsin-like activity (ChT-like, β5) which is thought to predominantly attack the carboxylic side of aromatic or bulky hydrophobic residues.[2] The observed specificities arise from the unique shape of the substrate binding pockets which are named S1−S4 in the N-terminal and S1′−S4′ in the C-terminal direction of a bound substrate, emanating from its cleavage position, which is the alcohol oxygen of Thr[1] (Thr[1]O$^{\gamma}$). Ligand parts reaching the substrate binding pockets follow a similar nomenclature where S is substituted by P.

The UPS is involved in several physiologically important cellular processes such as cell cycle progression, immune response, or signal transduction, which makes the CP an attractive therapeutic target for cancer and autoimmune disorders.[3−6] In fact, the dipeptidic boronic acid bortezomib and the tetrapeptidic epoxyketone carfilzomib are currently prescriptive drugs against various types of cancer, in particular relapsed multiple myeloma and mantle cell lymphoma.[5,6] Particularly, the β5 subunit is in the focus of therapeutic targeting, because its inhibition leads to high rates of apoptosis in tumor cells, which is accompanied by a protective effect on

Received: January 11, 2016
Accepted: April 25, 2016
Published: April 25, 2016

DOI: 10.1021/acschembio.6b00023
ACS Chem. Biol. 2016, 11, 1800−1804

Scheme 1. (a) Chemical Structures of the Tripeptidic Aldehyde Inhibitor 1 and Derivatives with Gradually Elongated P1 Residues 2−4 and the Analogue Substrate Derivates 5−7; (b) Visualization of the Molecular Recognition in a Mouse Trap Analogy;[a] (c) Molecular Dynamics Simulation of the Native β5 Subunit with Bound Inhibitors 1 and 2 and without Any Ligand[b]

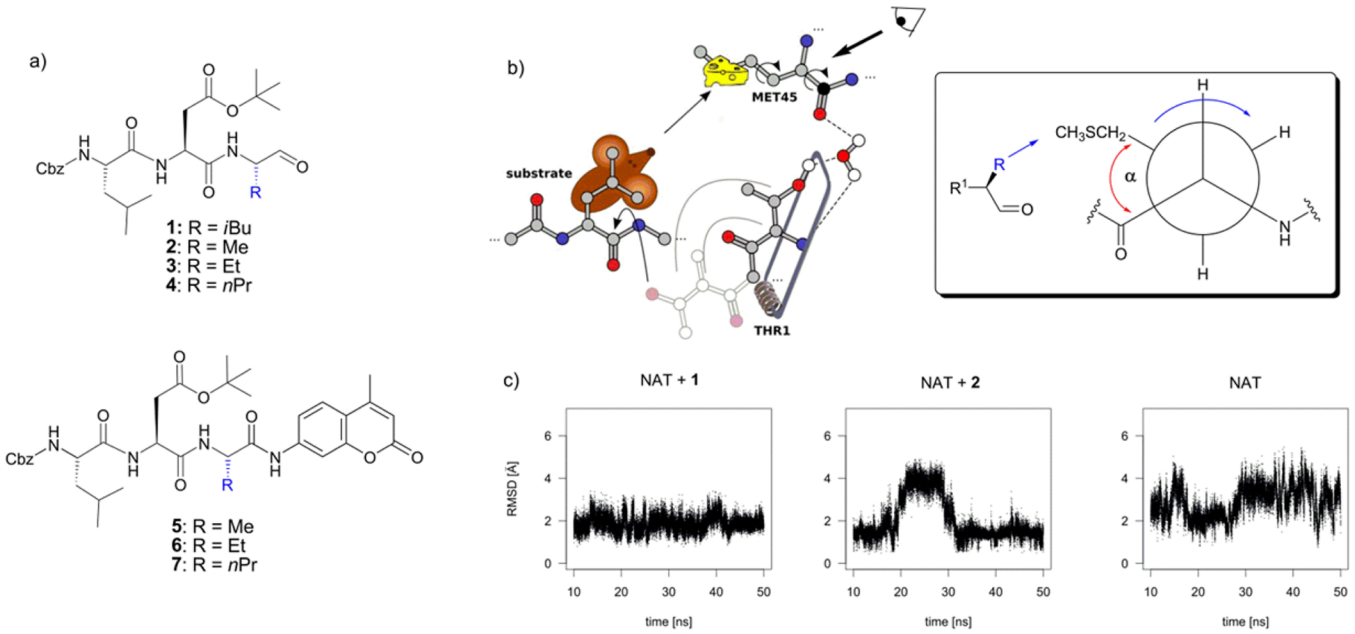

[a]Hydrophobic interactions between Met[45] and the ligand's P1 residue lead to conformational changes of the S1 subpocket's backbone. [b]The RMSD of the Met[45] side chain atoms relative to the starting frame is plotted over time. Calculations were done in VMD 2.9.

healthy cells.[7] In 2005, we identified the tripeptidic aldehyde BSc2118 (**1**; Scheme 1a) as a very potent ($IC_{50,\beta5}$ = 58 nM) and selective covalent CP inhibitor.[8] The special feature of **1** is a sterically demanding *tert*-butyl aspartate P2 residue, which discriminates inhibition against the majority of the protease environment. In a recent study, **1** shows cytotoxic effect against human tumor cells and efficacy in multiple myeloma xenografts.[9]

In this work, we investigated a ligand recognition mechanism leading to novel insights as a function of P1 residues on inhibitory activity as well as substrate hydrolysis. Our starting hypothesis was that ligand association and dissociation is influenced by hydrophobic interactions between a substrate's P1 residue and the highly flexible side chain of Met[45] within the proteasome's β5 subunit.[2] For example, in the **1**/proteasome complex,[8] Met[45] shows a dihedral angle α of about −167° compared to +48° in the native protein (Figure 1).[10] Interestingly, the dihedral angle is changed in a similar manner by a variety of inhibitors bearing P1 residues such as the ketoamide BSc4999[11] (α = −179°), the natural product syringolin A[12] (α = −175°), as well as the boronic acid bortezomib[13] (α = −174°), while inhibitors not occupying S1 like the recently reported indolo-phakellins[14] retain the native conformation (α = +51°) of Met[45]. A concerted mechanism may accelerate the association of substrates with large P1 residues due to a widening of the dihedral angle α of Met[45]. This induced fit was thought to imply a conformational change of the S1 subpocket's backbone, which would strengthen the coordination of a catalytically active water molecule and increase the nucleophilicity of Thr^1O^{γ}. An illustrative analogy for this triggered activation is the release of a mouse trap after the mouse touches the lure (Scheme 1b).

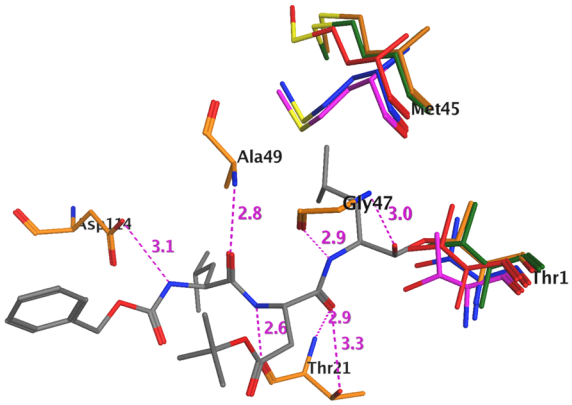

Figure 1. Comparison of the native (blue, α = +48°) and **1**-bound proteasome (gray in orange, α = −167°) structures detailing two distinct side chain conformations of Met[45]. Conformations of key residues Met[45] and Thr^1 are shown from crystal structures with peptidic inhibitors (bortezomib, green; BSc4999, red) and the nonpeptidic indolo-phakelline inhibitor (purple).

To gain detailed insights in the nature of the Met[45] flexibility depending on the size of the P1 residue (**1** and **2**), we performed a set of molecular dynamics simulations based on the crystal structure of the native yeast 20S proteasome (Scheme 1c). As expected, the side chain of Met[45] shows a high flexibility in absence of any ligand with an RMSD in the range of 2 to 6 Å. The simulation using the methyl derivative **2** was characterized by a switch between two stabilized states referring to the two distinct conformers of Met[45] as observed in the crystal structures. The in vitro testing of inhibitors derived from **1** with iteratively enlarged P1 residues (**2**−**4**; Scheme 1a) allowed a correlation between the size of a residue in the S1

DOI: 10.1021/acschembio.6b00023
ACS Chem. Biol. 2016, 11, 1800−1804

pocket and the resulting inhibitory activity. The length of the respective P1 residue has a direct influence on the dihedral angle α of Met[45] as shown in Scheme 1b. The experimental determination of β5-specific IC_{50} values revealed a continuous increase of the inhibitory activity from P1 = methyl ($IC_{50,\beta5}$ = 987 nM) via ethyl ($IC_{50,\beta5}$ = 362 nM) to *n*-propyl ($IC_{50,\beta5}$ = 219 nM) residues. While large P1 residues strengthen the inhibition by fixing the inhibitor in a specific receptor conformation, we questioned how this mechanism influences substrate hydrolysis.

Therefore, we used a substrate-based approach to identify Michaelis–Menten parameters of substrate conversion. We synthesized fluorogenic 7-amino-4-methylcoumarin (AMC) substrates (**5**–**7**; Scheme 1a, see SI for details), based on the original structure of **1** with iteratively elongated P1 residues. Experimental determination of the Michaelis constant K_M, the turnover rate k_{cat}, the maximum reaction velocity V_{max}, and the specificity constant (k_{cat}/K_M) was used to quantify the impact of a substrate-induced widening of the dihedral angle α of Met[45] on the β5 activity. To determine the kinetic properties of **5**–**7** and the widely used reference substrate for the ChT-like activity Suc-LLVY-AMC, we fluorometrically determined the respective initial velocities of the substrate cleavage dependent on the substrate concentration and analyzed the data *via* the Lineweaver–Burke plot (Figure 2). K_M can be interpreted as

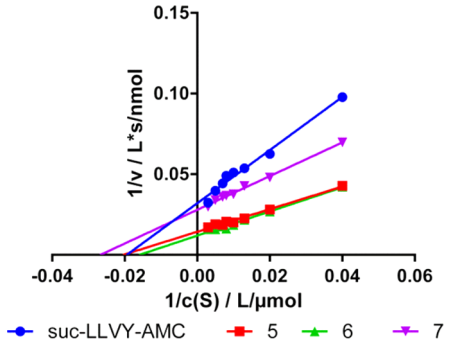

Figure 2. A double reciprocal Lineweaver–Burke plot of substrates **5**–**7** and Suc-LLVY-AMC. Each experiment was performed as quintuples in two independent measurements (n = 10).

the dissociation constant of the enzyme/substrate complex if the formation and dissociation step is much faster than product formation and thus describes the affinity of a substrate to the active site.[15] For all four substrates, the observed K_M values were found to be in a similar range from 40 μM for the propyl substrate **7** to 61 μM for the ethyl substrate **6**. This implies that all substrates, although they have a P1 length distribution from methyl over propyl to tyrosyl, share a similar affinity for the active site without any observable correlation of the P1 length and K_M, which is attributed to the flexibility of the Met[45] side chain. This flexibility may be able to shape a perfect S1 binding pocket for a variety of hydrophobic P1 residues. Substrates **5** and **6** with small P1 residues showed a 2-fold increase of V_{max} and k_{cat} compared to the substrates **7** and Suc-LLVY-AMC with bulky P1 side chains, which are caught in the mouse trap-like mechanism. This trend is also clearly demonstrated by the decrease of the specificity constant k_{cat}/K_M, which is a robust descriptor identifying the best substrate for a given enzyme.[16]

These findings contradict the postulated and so far unquestioned ChT-like activity of the β5 subunit. Following the ChT-like activity, the kinetic activation due to hydrophobic interactions of a substrate, and the Met[45] side chain, the turnover rate (k_{cat}) and the maximum reaction velocity (V_{max}) should increase with a growing P1 residue as increasing affinity is also observed for inhibitors. As a logical consequence, substrates with bulky hydrophobic or aromatic P1 residues were expected to be much better substrates than the methyl substrate **5**. Since substrates require a relatively high k_{off} rate to refresh the catalytic site, the swapped, non-native receptor conformation (α = −174°) is only favorable for inhibitors, whereas the near-native state (α = 48°) should be favorable for substrate conversion.

Thus, we conclude that the β5 subunit of the constitutive 20S proteasome favors a "small neutral amino acid preferring" (SNAAP) or "elastase-like" (E-like) over the ChT-like activity, and the classification should be expanded. The SNAAP or E-like activity of the 20S proteasome reported here was actually observed by Orlowski *et al.* in 1993 but at that time referred to an additional and unidentified active subunit.[17] Despite a report that the β7 subunit might be responsible for the SNAAP activity, which was not experimentally confirmed and presumed from structural data of the bovine 20S proteasome only, it was shown by mutational studies that any observed substrate cleavage is realized by the β1, β2, or β5 subunits.[18−20] In these studies, the identification of the SNAAP-responsible active site was not definite since it seemed to depend on the substrate sequence around a potential cleavage site and thus was assigned to all three active subunits.

The recently published structure of the murine immunoproteasome permits a new explanation of why the β5 subunit is responsible for this E-like activity. In immunoproteasomes, the β5 subunit (β5i) harbors a structurally different S1 pocket compared to its constitutive counterpart (β5c).[20] In β5c, the Met[45] side chain is flexible and points to the substrate binding channel, whereas in β5i it is oriented toward Gln[53] engaged in strong van der Waals interactions. In β5c, this Gln[53] residue is replaced by Ser, which cannot stabilize this orientation of Met[45] and thus leads to a much smaller S1 binding pocket. Because of the Met[45] flexibility, substrates with bulky P1 residues are able to reach the active site, but their hydrolysis is disfavored compared to substrates bearing a small hydrophobic side chain on this position. This discrimination may be due to major structural changes of the protein backbone that are necessary to enlarge the S1 pocket.[21] Substrate hydrolysis requires fast and dynamic structural changes, as the initial state has to be restored after every cleavage event. This induced fit may be beneficial for inhibiting the β5 active site in an irreversible or slowly reversible manner but hinders substrate clearance from the active site. This explains the experimental finding that inhibitors with iteratively enlarged P1 residues show increased inhibitory activities, whereas the velocity of hydrolytic cleavage of respective substrates with identical peptidic backbones decreases.

Additionally, the examination of the Lineweaver–Burke plots also brought to our attention a slight deviation from a strictly linear behavior for the propyl substrate **7** and more significantly for the reference substrate Suc-LLVY-AMC (Table 1).

One feasible explanation for this anomaly is the participation of at least one additional active site to contribute to the substrate cleavage. In a subsequent analysis, this "leakage" for **7** and Suc-LLVY-AMC was investigated by silencing the catalytic β5 subunit selectively. The 20S proteasome was preincubated with a high concentration (500 nM, about 10-fold IC_{50}) of inhibitor **1**. It is noteworthy that the aldehyde inhibitor **1** shows

DOI: 10.1021/acschembio.6b00023
ACS Chem. Biol. 2016, 11, 1800–1804

Table 1. Key Parameters of Substrate Conversion As Determined by Lineweaver−Burk Plot and Residual Activity of Different Substrates after Silencing the β5 Subunit

	5	6	7	Suc-LLVY-AMC
K_M (μM)	45.1	61.7	39.4	49.7
V_{max} (nM·s^{-1})	70.8	85.3	37.8	31.5
K_{cat} (1·s^{-1})	49.6	59.7	26.5	22.1
K_{cat}/K_M (L·μmol^{-1}·s^{-1})	1.1	1.0	0.7	0.4
residual activity (%)	0.5	0.4	1.2	12.0

no significant inhibitory activity against any other active site than β5 (see Supporting Information Figure 1). The hydrolytic activity dropped dramatically for **5** (0.5% of control) and **6** (0.4%), indicating that these substrates are exclusively cleaved by the β5 subunit. Substrate **7** showed a slightly higher remaining hydrolytic cleavage after the β5 knockout of 1.2%, which may be the reason for the observed deviation from a strict linear Lineweaver−Burke plot. Surprisingly, the reference substrate Suc-LLVY-AMC, which is used in the majority of β5 activity assays, showed a remaining activity of 12% using the same conditions. This is consistent with the obvious nonlinear behavior of the Lineweaver−Burke plot and questions the wide use of this substrate in proteasome assays. The analogue experiments performed with epoxomicin led to similar results with slight variations in residual activity due to a less favorable selectivity profile (see Supporting Information Table 3).

These findings are in accordance with the occasional use of the substrate Ac-WLA-AMC, which has been reported to be preferentially hydrolyzed by the β5c subunit, instead of Suc-LLVY-AMC in recent studies.[22]

Based on these results, it becomes obvious that the inverse correlation of inhibition and hydrolysis strength arises from the same phenomenon. Reversible inhibitor binding can be defined by the ratio $K_i = k_{off}/k_{on}$; thus the mouse trap analogy implies an increased *on* rate (depicted as the "cheese trigger") as well as a decreased *off* rate ("caught by trap") if activated by large residues. Use of this mechanism is especially valuable for the development of potent irreversible or slowly reversible binding inhibitors and actually has been applied unknowingly. The native state which is only accessible using small substituents at P1 leads to the opposite findings, which can be classically described by the Michaelis−Menten approach. Increasing P1 residues lead to increased hydrophobic interactions in S1, thus strengthening inhibition as well as the corresponding substrate affinity quantified by K_M. Due to the activation of the mouse trap, substrate dissociation is hindered, leading to a lower turnover number k_{cat}. This exemplifies that K_M values solely can, at least in some cases, not describe substrate conversion preferences of enzymes appropriately. Mechanistic comparability of inhibition and hydrolysis is particularly warranted as both events involve covalent addition to the catalytic Thr[1].

Unselective cleavage of the established reference substrate may be critical when Suc-LLVY-AMC is used to rank the selectivity and potency of inhibitors for the β5 subunit. For this reason, substrate **5**, Z-Leu-Asp(O*tBu*)-Ala-AMC, is preferable for these applications, and the replacement of Suc-LLVY-AMC by **5** is recommended.

■ ASSOCIATED CONTENT

Supporting Information

The Supporting Information is available free of charge on the ACS Publications website at DOI: 10.1021/acschembio.6b00023.

Synthesis, molecular dynamics simulation, *in vitro* proteasome assays, compound characterization data, and references (PDF)

■ AUTHOR INFORMATION

Corresponding Author

*E-mail: schmidt_boris@t-online.de.

Author Contributions

[‖]These authors contribute equally to this work.

Notes

The authors declare no competing financial interest.

■ ACKNOWLEDGMENTS

This work was supported by the Deutsche Forschungsgemeinschaft (DFG), Germany (GRK1657) and by the Hans und Ilse Breuer Stiftung.

■ REFERENCES

(1) Hershko, A., Leshinsky, E., Ganoth, D., and Heller, H. (1984) ATP-dependent degradation of ubiquitin-protein conjugates. *Proc. Natl. Acad. Sci. U. S. A. 81*, 1619−1623.

(2) Borissenko, L., and Groll, M. (2007) 20S proteasome and its inhibitors: crystallographic knowledge for drug development. *Chem. Rev. 107*, 687−717.

(3) Driscoll, J., Brown, M. G., Finley, D., and Monaco, J. J. (1993) MHC-linked LMP gene products specifically alter peptidase activities of the proteasome. *Nature 365*, 262−264.

(4) Voorhees, P. M., Dees, E. C., O'Neil, B., and Orlowski, R. Z. (2003) The Proteasome as a Target for Cancer Therapy. *Clin. Cancer Res. 9*, 6316−6325.

(5) Kortuem, K. M., and Stewart, A. K. (2013) Carfilzomib. *Blood 121*, 893−897.

(6) Kane, R. C., Farrell, A. T., Sridhara, R., and Pazdur, R. (2006) United States Food and Drug Administration approval summary: bortezomib for the treatment of progressive multiple myeloma after one prior therapy. *Clin. Cancer Res. 12*, 2955−2960.

(7) Meiners, S., Ludwig, A., Stangl, V., and Stangl, K. (2008) Proteasome inhibitors: Poisons and remedies. *Med. Res. Rev. 28*, 309−327.

(8) Braun, H. A., Umbreen, S., Groll, M., Kuckelkorn, U., Mlynarczuk, I., Wigand, M. E., Drung, I., Kloetzel, P.-M., and Schmidt, B. (2005) Tripeptide Mimetics Inhibit the 20 S Proteasome by Covalent Bonding to the Active Threonines. *J. Biol. Chem. 280*, 28394−28401.

(9) Zang, M., Li, Z., Liu, L., Li, F., Li, X., Dai, Y., Li, W., Kuckelkorn, U., Doeppner, T. R., Hermann, D. M., Zhou, W., Qiu, L., and Jin, F. (2015) Anti-tumor activity of the proteasome inhibitor BSc2118 against human multiple myeloma. *Cancer Lett. 366*, 173−181.

(10) Groll, M., Ditzel, L., Lowe, J., Stock, D., Bochtler, M., Bartunik, H. D., and Huber, R. (1997) Structure of 20S proteasome from yeast at 2.4A resolution. *Nature 386*, 463−471.

(11) Voss, C., Scholz, C., Knorr, S., Beck, P., Stein, M. L., Zall, A., Kuckelkorn, U., Kloetzel, P.-M., Groll, M., Hamacher, K., and Schmidt, B. (2014) α-Keto Phenylamides as P1′-Extended Proteasome Inhibitors. *ChemMedChem 9*, 2557−2564.

(12) Groll, M., Schellenberg, B., Bachmann, A. S., Archer, C. R., Huber, R., Powell, T. K., Lindow, S., Kaiser, M., and Dudler, M. (2008) A plant pathogen virulence factor inhibits the eukaryotic proteasome by a novel mechanism. *Nature 452*, 755−758.

DOI: 10.1021/acschembio.6b00023
ACS Chem. Biol. 2016, 11, 1800−1804

(13) Groll, M., Berkers, C. R., Ploegh, H. L., and Ovaa, H. (2006) Crystal structure of the boronic acid-based proteasome inhibitor bortezomib in complex with the yeast 20S proteasome. *Structure 14*, 451−456.
(14) Beck, P., Lansdell, T. A., Hewlett, N. M., Tepe, J. J., and Groll, M. (2015) Indolo-Phakellins as β5-Specific Noncovalent Proteasome Inhibitors. *Angew. Chem., Int. Ed. 54*, 2830−2833.
(15) Chen, W. W., Niepel, M., and Sorger, P. K. (2010) Classic and contemporary approaches to modeling biochemical reactions. *Genes Dev. 24*, 1861−1875.
(16) Eisenthal, R., Danson, M. J., and Hough, D. W. (2007) Catalytic efficiency and kcat/KM: a useful comparator? *Trends Biotechnol. 25*, 247−249.
(17) Orlowski, M., Cardozo, C., and Michaud, C. (1993) Evidence for the presence of five distinct proteolytic components in the pituitary multicatalytic proteinase complex. Properties of two components cleaving bonds on the carboxyl side of branched chain and small neutral amino acids. *Biochemistry 32*, 1563−1572.
(18) Unno, M., Mizushima, T., Morimoto, Y., Tomisugi, Y., Tanaka, K., Yasuoka, N., and Tsukihara, T. (2002) The Structure of the Mammalian 20S Proteasome at 2.75 Å Resolution. *Structure 10*, 609−618.
(19) Dick, T. P., Nussbaum, A. K., Deeg, M., Heinemeyer, W., Groll, M., Schirle, M., Keilholz, W., Stevanović, S., Wolf, D. H., Huber, R., Rammensee, H.-G., and Schild, H. (1998) Contribution of Proteasomal β-Subunits to the Cleavage of Peptide Substrates Analyzed with Yeast Mutants. *J. Biol. Chem. 273*, 25637−25646.
(20) Huber, E. M., Basler, M., Schwab, R., Heinemeyer, W., Kirk, C. J., Groettrup, M., and Groll, M. (2012) Immuno- and Constitutive Proteasome Crystal Structures Reveal Differences in Substrate and Inhibitor Specificity. *Cell 148*, 727−738.
(21) Huber, E. M., and Groll, M. (2012) Identifizierung eines Sulfonamids als β1/β2-spezifischer Proteasomligand durch kristallographisches Screening. *Angew. Chem., Int. Ed. 51*, 8708−8720.
(22) Blackburn, C., Gigstad, K. M., Hales, P., Garcia, K., Jones, M., Bruzzese, F. J., Barrett, C., Liu, J. X., Soucy, T. A., Sappal, D. S., Bump, N., Olhava, E. J., Fleming, P., Dick, L. R., Tsu, C., Sintchak, M. D., and Blank, J. L. (2010) Characterization of a new series of non-covalent proteasome inhibitors with exquisite potency and selectivity for the 20S β5-subunit. *Biochem. J. 430*, 461−476.

DOI: 10.1021/acschembio.6b00023
ACS Chem. Biol. 2016, 11, 1800−1804